energies

MDPI

Article

Optimal Allocation of Static Var Compensators in Electric Power Systems

Martin Ćalasan [1,*], Tatjana Konjić [2], Katarina Kecojević [1] and Lazar Nikitović [1]

1 Faculty of Electrical Engineering, University of Montenegro, 81000 Podgorica, Montenegro; katarinakecojevic@gmail.com (K.K.); lazar.nikitovic.norsk@gmail.com (L.N.)

2 Faculty of Electrical Engineering, University of Sarajevo, 71000 Sarajevo, Bosna and Herzegovina; tatjana.konjic8@gmail.com

* Correspondence: martinc@ucg.ac.me; Tel.: +382-67615237

Received: 19 May 2020; Accepted: 12 June 2020; Published: 21 June 2020

check for updates

Abstract: In the current age, power systems contain many modern elements, one example being Flexible AC Transmission System (FACTS) devices, which play an important role in enhancing the static and dynamic performance of the systems. However, due to the high costs of FACTS devices, the location, type, and value of the reactive power of these devices must be optimized to maximize their resulting benefits. In this paper, the problem of optimal power flow for the minimization of power losses is considered for a power system with or without a FACTS controller, such as a Static Var Compensator (SVC) device The impact of location and SVC reactive power values on power system losses are considered in power systems with and without the presence of wind power. Furthermore, constant and variable load are considered. The mentioned investigation is realized on both IEEE 9 and IEEE 30 test bus systems. Optimal SVC allocation are performed in program GAMS using CONOPT solver. For constant load data, the obtained results of an optimal SVC allocation and the minimal value of power losses are compared with known solutions from the literature. It is shown that the CONOPT solver is useful for finding the optimal location of SVC devices in a power system with or without the presence of wind energy. The comparison of results obtained using CONOPT solver and four metaheuristic method for minimization of power system losses are also investigated and presented.

Keywords: power system losses; SVC devices; wind energy; optimal location; CONOPT solver; metaheuristic methods

1. Introduction

Today, life without electricity is almost impossible to imagine. Generated electricity (active and reactive power) is usually transmitted over long distances to end users. However, due to the AC transmission line impedance and the voltage drop across the line, power losses always exist [1,2].

Modern power systems, besides classic generating units, consist of many renewables [3]. There are also a lot of different devices based on power electronics, an example being Flexible Alternating Current Transmission System (FACTS) devices. At the moment, FACTS devices are used as the most advanced reactive energy compensation devices [2]. They are also used to solve various problems in the power system such as power system stability, power transfer capacity, voltage profile, power system efficiency, and so on [2]. This paper, in general, deals with one of the most used types of FACTS devices, known as SVC devices (Static VAr Compensator).

The SVC is the first FACTS device to be developed. This device connects in parallel to the system and is essentially a combination of parallel-connected capacitors (fixed or variable capacity) and coils so that it can operate in either inductive or capacitive mode [2]. Therefore, it is dominantly used to regulate voltage and reactive power in a power system. Furthermore, these devices can regulate, i.e., produce and absorb reactive power over a wide range. As they are one of the cheaper FACTS devices, they are often observed in power studies. In the available literature, we can find many different studies on FACTS devices, especially on SVC devices, and their allocation in power systems with or without the presence of renewables [3–25]. For example, the coordination of SVC devices and other FACTS devices for the management of power flow is presented in [3]. Furthermore, the optimal placement and parameter setting of SVC devices for solving power system stability problems, the damping system-wide low-frequency oscillations, as well as power system loadability is presented in [4–11]. The loadability problem is often investigated along with the optimal system control for the minimization of total power system losses [11]. The minimization of total power losses is one of the main goals of the implementation of FACTS devices in power networks; for this reason, almost all the papers dealing with FACTS devices observe this problem [11–14]. Finding the optimal setting of all control variables of FACTS devices, for different purposes, is investigated in [15–22]. In the literature, we can also find research looking into the improvement of voltage profiles in distribution networks with renewable power sources [15,17], the maximization of photovoltaic hosting capacities that minimize system operating costs [16], the improvement in the reconstruction of power systems with wind generation [17], voltage profile enhancement [22], power quality improvement [24,25], and so on.

The enhancement of the voltage profile by using FACTS devices is strongly related to power loss minimization [15,22]. This fact is investigated in detail in [22], observing both IEEE 9 and IEEE 30 bus systems. However, in [22], the authors analyze voltage profile enhancement and power loss minimization only at constant load (a one-time step), which is not a realistic case. On the other side, in [22], some data mismatching is evident. For example, system data do not correspond to the graphical view of analyzed networks, and so on. Also, the obtained results of optimal power system losses without SVC devices differ from results evident in many of the previously published papers that deal with optimal power flow (OPF). In [22], it is observed that the minimal value of power losses in the IEEE 30 test bus network, without SVC devices, is 2.86 MW, while in [26–30], the value of power system losses is about 3.1 MW or higher. The same situation occurs with the IEEE 9 test bus system. On the other side, in [31], the authors analyze the impact of SVC devices on a IEEE 24 test bus system with three wind generators without any discussion about the power loss variation, the optimal node for an SVC or similar device.

Beside large power systems, the use of FACTS devices is also investigated for microgrid systems [32–37]. In general, microgrids are small energy grids in terms of scale, power, voltage level, and contain a different generator unit that can provide an adequate energy supply to demand [36]. This design, in grid-connected and islanding modes, with SVC devices can significantly improve voltage stability, enhance power factor, reduce power system losses, mitigate the harmonic distortion, and so on [37].

Different FACTS devices and power system stabilizers (PSS) can be also used for damping power system oscillations [38,39]. A PSS in control devices provides maximum power transfer and thus improves power system stability [40]. Disturbances occurring in a power system cause electromechanical oscillations, and PSS have been widely used to damp these oscillations [41]. By introducing additional signals into the excitation controllers of the generators, PSS can increase the damping torque of a system's local mode [42]. PSS are used as additional control devices to provide extra damping. The basic role of an SVC device is to control reactive power flow and fluctuations in system voltage. A supplementary role added to an SVC is to increase the power system damping. In order to enhance the damping of system oscillations, an SVC can be designed to modulate its bus voltage, especially for inter-area modes [43].

The abovementioned studies have observed many different types of power systems. In some cases, the authors observed standard IEEE test bus systems [4,8,12,13], while in other papers, authors observed distribution systems [15,16]. Also, the problem of the optimal location of FACTS devices is predominantly solved by using some metaheuristic techniques. The techniques that can be found in the literature are Particle Swarm Optimization (PSO) [4,19,20], Genetic Algorithm (GA) [5,10,20], Hybrid Imperialist Competitive Algorithm genetic Algorithm (HICAGA) [11], Whale Optimization Algorithm (WOA) [12], Differential Evolution (DE) [12], Grey Wolf Optimization (GWO) [12], Quasi-Opposition based Differential Evolution (QODE) [12], Quasi-Opposition based Grey Wolf Optimization (QOGWO) [12], Differential Search (DS) [13], Simulated Annealing (SA) [20], Pattern Search (PS) [20], Backtracking Search Algorithm (BSA) [20], Gravitational Search Algorithm (GSA) [20], and Reproduction Optimization (ARO) [20]. An updated review of papers dealing with the optimal placement of different FACTS devices in power energy systems using metaheuristic optimization techniques is presented in [21]. Besides metaheuristic methods, the optimal placement of SVC devices can be also solved by using the Newton–Raphson method [22], as well as by using non-traditional optimization techniques [23]. Many existing optimization methods dealing with the optimal location of SVC devices to obtain better system performance, such as smaller power system losses, point to the necessity of further research in this scientific field.

In this paper, we present the use of a CONOPT solver [26,31,44,45] embedded in the Generalized Algebraic Modeling Systems (GAMS) software package for this issue. The advantage of a CONOPT solver embedded in GAMS over other optimization techniques is its high-speed processing, as well as the fact that it always converges to the same optimal solution for any program starting [26]. This paper also presents addition comparisons of the CONOPT solver and four metaheuristic methods (PSO, GSA—Gravitational search algorithm [46,47], ABC—Artificial bee colony algorithm [29], and DE [12,48–50]). The optimal location of SVC devices is analyzed in IEEE 9 and IEEE 30 test systems. However, unlike [22], in this paper, four cases are analyzed—the optimal SVC location in a power system with constant load; the optimal SVC location in a power system with variable load; the optimal SVC location in a power system with variable load in the presence of wind energy, and the impact of location of both a wind generator and SVC devices on power system losses. To the best of our knowledge, this kind of research has not been presented in any of the previously published papers.

The main contributions of this paper are as follows:

- The comparison of four metaheuristic algorithms applied to single-objective optimal power flow (with the objective function of minimization of power system losses) is presented and tested on both IEEE 9 and IEEE 30 test bus systems and comparison is made with similar studies in the literature;
- The comparison of minimum power system losses obtained using a CONOPT solver and the metaheuristics algorithms is presented;
- The impact of SVC location on power system losses is analyzed in both IEEE 9 and IEEE 30 test bus systems;
- The impact of the limited reactive power of SVC devices on power system losses is also analyzed in the same test systems;
- The impact of SVC location on power system losses in power networks with renewables is analyzed;
- The impact of different wind power generator connections in power networks on the SVC location is tested;
- For constant load data, the results obtained using the Newton–Rapson method for optimal SVC location and the minimal value of power losses are compared with known solutions from the literature

The remainder of the paper is organized as follows. Section 2 gives basic information about SVC devices. The main equations related to the OPF problem are presented in Section 3. Basic information about the GAMS-CONOPT solver and a comparison of the CONOPT solver with metaheuristic algorithms are presented in Section 4. The impact of SVC location on power system losses that have been analyzed in four basic cases, their variations, and the simulation results are given in Section 5. Concluding statements and directions for future work are presented in Section 6.

2. SVC Devices

The general circuit structure of an SVC is presented in Figure 1 [1,2]. As can be seen, and as noted earlier, an SVC is composed of a fixed capacitor and thyristor-controlled reactor. The equivalent susceptance B_{SVC} of the SVC device is determined by the firing angle α of the thyristor. The equivalent susceptance, and the reactive power provided by SVC, in i-th node, can be expressed as follows:

$$B_{SVC} = B_L(\alpha) + B_C,\ B_L(\alpha) = -\frac{1}{\omega L}\left(1 - \frac{2\alpha}{\pi}\right),\ B_C = \omega C \tag{1}$$

$$Q_{SVC} = -V_i^2 B_{SVC} \tag{2}$$

where L and C are the inductance of the reactor and the capacitance of the capacitor, respectively, and V_i is the voltage value in node i. If the system load is capacitive, the SVC uses thyristor-controlled coils to consume reactive power from the system, and when the load is predominantly inductive, the SVC uses parallel-coupled capacitors and produces reactive energy, thus improving voltage conditions. The basic task of an SVC is to achieve fast and continuous control.

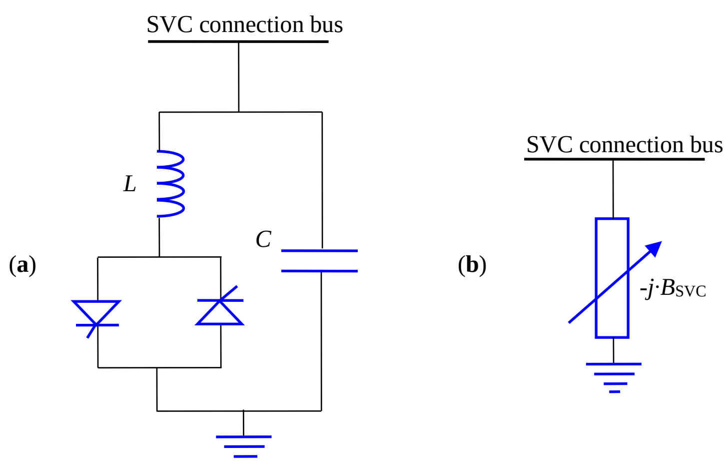

Figure 1. A Static Var Compensator (SVC). (**a**) circuit structure and (**b**) equivalent model.

3. Optimal Power Flow Formulation

Optimal power flow is one of the most crucial problems in power systems; it is used to determine the optimal settings for control variables while respecting various constrains [51].

The standard formulation of an OPF problem is:

$$\begin{array}{c} Minimize\ J(x,u) \\ g(x,u) = 0 \\ h(x,u) \leq 0 \end{array} \tag{3}$$

where u is a vector of independent or control variables (such as active power generation at the PV buses except the slack bus, voltage magnitudes at PV buses, tap settings of the transformers), x is a vector of dependent or state variables (such as active power at slack bus, voltage magnitude at PQ busses, reactive power output of all generator units), J is the system's optimization goal—objective function (such as total fuel cost, total emission, total power losses, voltage deviation, etc.), g is set of equality equation, and h is set of the inequality constraints.

The equality constraints of the OPF can be represented as follows:

$$\begin{aligned} P_{Gi} - P_{Di} - V_i \sum_{j=1}^{NB} V_j \Big[G_{ij} \cos\Big(\theta_{ij}\Big) + B_{ij} \sin\Big(\theta_{ij}\Big) \Big] = 0 \\ Q_{Gi} - Q_{Di} - V_i \sum_{j=1}^{NB} V_j \Big[G_{ij} \sin\Big(\theta_{ij}\Big) + B_{ij} \cos\Big(\theta_{ij}\Big) \Big] = 0 \end{aligned} \tag{4}$$

where $\theta_{ij} = \theta_i - \theta_j$, θ_i and θ_i are phase angle of voltage in node i and j, respectively, NB is the number of buses, V_i and V_j are voltages in node i and j, respectively, P_{Gi} is the active power generation in node i, Q_{Gi} is the reactive power generation in node i, P_{Di} is active power of demand in node i, Q_{Di} is reactive power of demand in node i, and G_{ij} and B_{ij} are elements of admittance matrix representing conductance and susceptance between buses i and j, respectively.

The inequality constraints of the OPF reflect the limits of the devices present in the power system. The main inequality constraints are as follows:

- Generator constraints:

$$\begin{aligned} V_{G_i}^{\min} \le V_{G_i} \le V_{G_i}^{\max},\ i = 1,\ \ldots,\ \mathrm{NG} \\ P_{G_i}^{\min} \le P_{G_i} \le P_{G_i}^{\max},\ i = 1,\ \ldots,\ \mathrm{NG} \\ Q_{G_i}^{\min} \le Q_{G_i} \le Q_{G_i}^{\max},\ i = 1,\ \ldots,\ \mathrm{NG} \end{aligned} \tag{5}$$

- Transformer constraints:

$$T_i^{\min} \le T_i \le T_i^{\max},\ i = 1,\ \ldots, NT \tag{6}$$

- Security constraints:

$$\begin{aligned} & V_{L_i}^{\min} \le V_{L_i} \le V_{L_i}^{\max},\ i = 1,\ \ldots, NL \\ & \mathrm{S}_{\mathrm{l_i}} \le \mathrm{S}_{l_i}^{\max} \end{aligned} \tag{7}$$

In the above Equations (5)–(7), NG refers to the number of generators, NT is the number of transformers, NL is the number of lines, T is transformer-tap settings ought, V_L is line voltage, V_G is generator voltage, and S_l is line power.

Some OPF objective functions are:

- Minimization of total fuel cost:

$$OF = \sum_{i=1}^{NG} \Big(a_i P_{G_i}^2 + b_i P_{G_i} + C_i \Big) \tag{8}$$

where a_i, b_i, and c_i are the cost coefficients of generator i.

- Minimization of total emission:

$$OF = \sum_{i=1}^{NG} \Big(\gamma_i P_{G_i}^2 + \beta_i P_{G_i} + \alpha_i + \xi_i e^{\lambda_i P_{G_i}} \Big) \tag{9}$$

where γ_i, β_i, α_i, ξ_i, and λ_i are the emission coefficients of unit i

- Voltage deviation minimization:

$$OF = \sum_{i=1}^{NG} |V_i - 1| \tag{10}$$

- Total active power loss minimization:

$$OF = \sum_{i=1}^{NB} \left(P_{G_i}\right) - \sum_{i=1}^{NB} \left(P_{D_i}\right) \tag{11}$$

In an OPF problem, one (single-objective OPF) or more (multi-objective OPF) objective functions can be optimized at the same time.

4. Comparison of Metaheuristics Methods and Solver CONOPT for OPF Problem Solving

The optimal placement of SVC devices in power networks requires the optimal power flow problem solving. As noted in the Introduction, different metaheuristic methods can be used for the optimal placement of SVC devices in power networks. Firstly, this section gives a short review of the advantages and drawbacks of metaheuristic methods for OPF problem solving. Secondly, basic information about program GAMS and solver CONOPT is presented. Thirdly, comparisons of the results obtained by using three metaheuristic methods and solver CONOPT for the minimization of power system losses are presented.

4.1. Short Comments on Metaheuristic Methods for OPF

The fast development of power systems and the power market has introduced the need to optimize many practical problems, and make operation, planning, and maintenance as efficient as possible. One optimization problem that is continuously present in the power system is the optimal power flow (OPF) problem. OPF was first discussed by Carpentier [52].

OPF has been previously evaluated in a complex, non-linear, and non-convex problem mix-integer and highly constrained fashion. Therefore, the need for new methods to solve the problem has risen. Classical optimization methods such as Newton's methods, linear programming, nonlinear programming, quadratic programming, and many others [53], due to their difficulties of differentiability and nonlinearity, are not able to a provide global optimum and often just provide a local solution. To overcome this issue, a solution has been found in metaheuristics. The term metaheuristic, first introduced by Glover in [54] derives from two words—*heuriskein* (ancient Greek) or *heurisricus* (Latin) means "to find out, discover" and *meta* (ancient Greek) means "beyond, in an upper level". Significant development of different methods in the field of metaheuristics have occurred in the last two decades. These methods, using simple mathematical rules, are designed to search a large solution space and find a sufficiently good candidate solution (global or near-global solution) iteratively in a reasonable computation time. Metaheuristic methods are mainly based on phenomenon in natural, biological, physical, and chemical systems. Therefore, there are a plethora of different metaheuristic methods [55,56].

If the classical optimization method is used to solve optimizations problems, it is necessary that the defined objective function should be differentiable and continuous. In metaheuristics, there are no restrictions for objective functions, which is one of its main advantages. Metaheuristics can be used for various complex optimization problems considering different objective functions and constrains but it never guarantees the optimal solution. There are a lot of different metaheuristic methods that can be applied to different optimization problems. However, some can be used to solve some specific problems very well, while not being appropriate for other types of problems. Therefore, it is always advisable to test a variety of metaheuristics methods for a specific problem and compare the results. The two main drawbacks of metaheuristics methods are that they do not guarantee that a globally optimal solution can be found, and that the solution found is dependent on the initial condition.

Metaheuristics has been recognized as one of the most successful approaches to solving large-scale optimization problems in power systems [57], including OPF problems [51,58,59]. In recent years, to overcome specific limitations of the underlying metaheuristics, a new field in metaheuristics has appeared combining the ideas of two or more metaheuristic method, called a hybrid metaheuristic [60].

4.2. Basic Information about CONOPT Solver Embedded in GAMS

The GAMS is a modeling tool for mathematical programming and optimization purposes. It can be used to solve different types of optimization problems [45]. This is a consequence of the fact that a large number of solvers for mathematical programming models, such as Linear Programming, Nonlinear Programming, Linear Regression and so on, are embedded in GAMS.

The CONOPT solver embedded in GAMS is well-suited for models with very nonlinear constraints, large models, models described with smooth functions, and so on. Finally, the CONOPT solver is an unequaled GAMS solver in terms of requested computation time. Namely, it has implemented three active-set methods and algorithmic switches that automatically detect the best method for problem-solving [61]. For this reason, in [61] is noted that the CONOPT solver is a high-speed solver.

4.3. Results of Comparisons

Four metaheuristic methods were applied on an OPF problem and the obtained results were compared in terms of copulation time, accuracy, and impact of system dimension with GAMS/CONOPT [21]. It was shown that the CONOPT solver embedded in GAMS provides an efficient and accurate solution, and that results are equal or better than those obtained using other optimization techniques.

In this paper, PSO, GSA, ABC, and DE algorithms were applied to OPF problem in both IEEE 9 and IEEE 30 test bus systems in order to further investigate some performances of CONOPT over metaheuristics algorithms. The objective function was power loss minimization. The basic PC parameters in this research were: 2.5 GHz Intel Core i7 and 8 GB RAM. The population size was set to 100 in each algorithm. For both observed IEEE test systems and each algorithm, 50 runs were performed, and the maximal iteration was set to 1000.

The change of the OPF objective function during the iterative procedure and the multiple runs of PSO, GSA, ABC, and DE algorithms in IEEE 9 test bus system are presented in Figure 2. Comparing OF values obtained by four metaheuristic algorithms, it is evident that DE and ABC algorithms are more stable, converge faster, and after 1000 iterations, end in the same OF value for multiple runs.

The values of OF in the first 10 iterations for multiple runs in case of the same four metaheuristics (PSO, GSA, ABC, DE) applied to the OPF problem in the IEEE 30 test bus system are presented in Figure 3. It can be noticed that OF has different values at the beginning of the iterative procedure in each run. In comparison with other observed algorithms, DE shows a smaller value of initial OF for multiple runs.

For the IEEE 9 test bus system, the maximal, mean, and minimal values of OF for all runs during the iterative procedure are presented in Figure 4. Different algorithms require a different number of iterations to reach an appropriate convergence. The ABC algorithm has the best convergence characteristics. The DE algorithm shows similar behavior to the ABC algorithm regarding convergence characteristic in this case. Both ABC and DE algorithms converge to the best solution among the others in less iterations.

The values of OF in the 1st, 50th, and 300th iteration, for each run and for both the IEEE 9 and IEEE 30 test bus systems, are presented in Figure 5a,b, respectively. It is evident that the chosen algorithms, although after a large number of iterations, do not converge to the same value. Convergence curves of ABC and DE algorithms are smoother than the curves of the PSO and GSA algorithms. The ABC and DE algorithms show similar and stable convergence in the 50th iteration and especially in 300th iteration for all 50 runs. The PSO algorithm has the worst convergence characteristics, with many variations in a wider range.

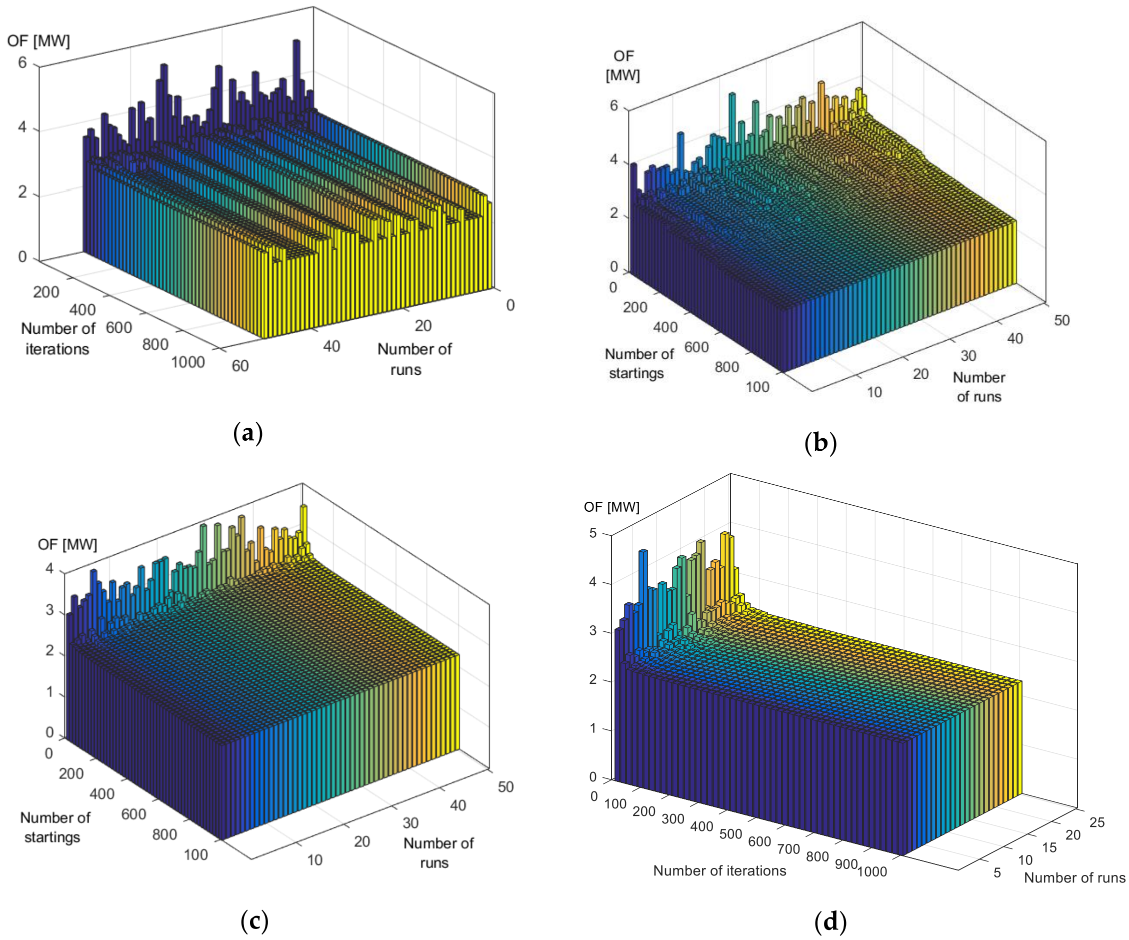

Figure 2. Change of optimal flow (OF) during the iterative procedure in multiple runs for the IEEE 9 test system (**a**) PSO, (**b**) GSA, (**c**) ABC, and (**d**) DE.

A summary of the obtained results regarding the best solution, the number of iterations needed to achieve the best solution, and the computation time for the four applied algorithms in both IEEE 9 and IEEE 30 test systems is given in Table 1. In addition, CONOPT results regarding the best solution and computation time are also given in Table 1. As the minimum problem consideration, the underline-bold value of power losses presents the best value while the bold value presents the worst. The DE algorithm provides the best solution and the total power losses in IEEE 30 is 2.994 MW, while the PSO algorithm provides the worst one, with 3.39 MW in total power losses. Active losses are reduced from 3.39 MW to 2.994 MW, that is, 11.68%. Because IEEE 9 is a small system, there are no visible differences between the algorithms. However, the best solution is achieved again by the DE algorithm. Regarding the computation time, it is interesting to notice that even though ABC and DE algorithms have very similar solutions (IEEE 9—ABC power system losses (P_{loss}) = 2.317 MW and DE P_{loss} = 2.316 MW; IEEE 30—ABC P_{loss} = 2.995 and MW and DE P_{loss} = 2.994 MW) and number of iterations are higher in the case of DE (e.g., in IEEE 30, DE needs 750 iterations while ABC needs 600), computation time is considerably less in the case of DE for both systems (e.g., in IEEE 30 DE needs 247.5 s for 750 iterations while ABC needs 420 s for 600 iterations). Therefore, in this comparison, DE beats the other meta-heuristics algorithms.

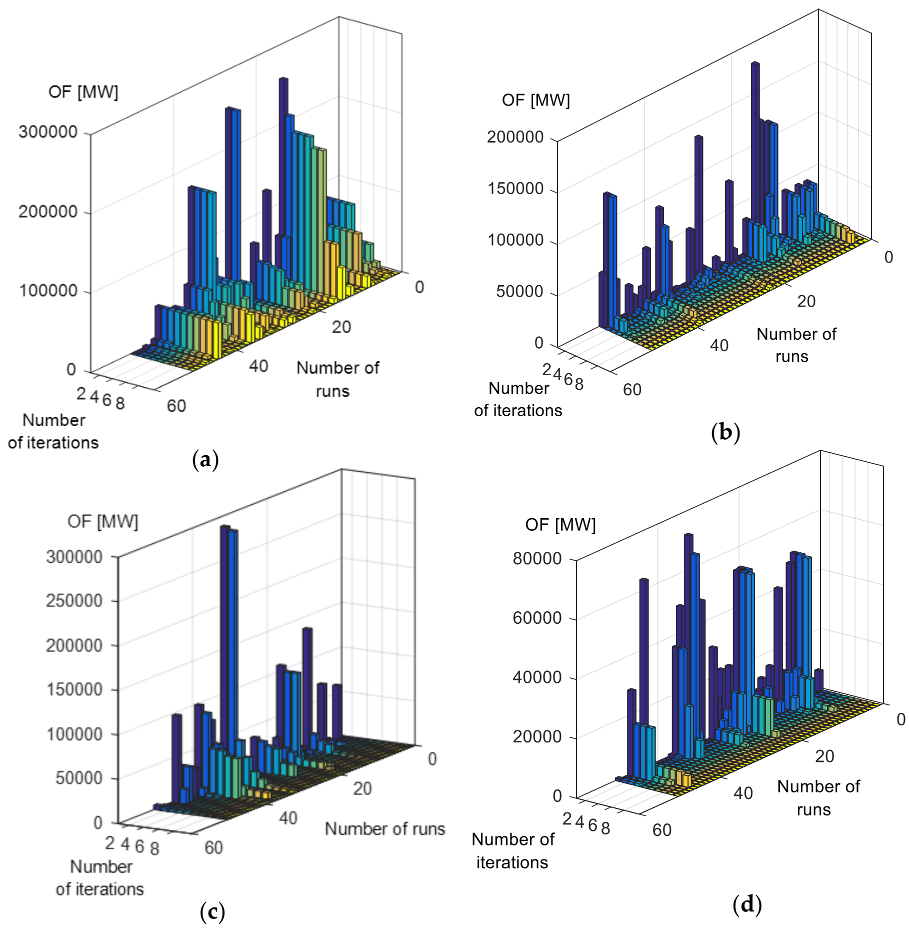

Figure 3. Change of OF during the first 10 iterations in multiple runs for the IEEE 30 test bus system: (**a**) PSO, (**b**) GSA, (**c**) ABC, and (**d**) DE algorithm.

The value of total power losses obtained using the CONOPT solver for the IEEE 9 test bus system is 2.3157972 MW, while for the IEEE 30 test bus system it is 2.9937435 MW. The results regarding total power losses are not much better than those obtained by DE (2.316 MW for IEEE 9 and 2.994 MW for IEEE 30). In order to obtain better results in terms of total power losses, the metaheuristic algorithms need a large number of iterations (DE needs 750 iterations for IEEE 30 and 320 iterations for IEEE 9) and computation time is 8.32 s for IEEE 9 and 247.5 s for IEEE 30, while CONOPT needs 0.073 s for IEEE9 and 0.092 s for IEEE 30 to achieve the best solution.

In [26], the authors also show that the requested computation time of the CONOPT solver embedded in GAMS is significantly lower compared to other techniques. On the other hand, the CONOPT solver embedded in GAMS always converges to the same optimal solution for each run. However, to make comparison with the research work of other authors, it is hard to find similar conditions in the literature review when solving OPF problems by different algorithms in the same test systems. Authors in [62] analyze different methods for the OPF problem with multi-objective and single objective functions in the IEEE 30 test system; in the case of single objective OF, the total power losses obtained by PSO algorithms are 3.629 MW, which is higher than in this research. In [63], the authors obtained total power losses of 3.24 MW in the IEEE 30 test system by DE with a population size of 100 and 300 maximum iterations. According to the results shown in Table 1, the total power losses obtained by DE in the IEEE 30 system are 2.994 MW, with the same population size of 100, but after 750 iterations. In the 300th iteration for IEEE 30, total power losses are 3.01MW (Figure 5b that is little less than in [63]). In [64], the authors obtained total power losses of 3.1216 MW in the IEEE 30 test system by ABC and 3.0917 MW by improved ABC (IABC) with a population size of 100 and 200 maximum iterations. In Table 1, total power losses are 2.995 MW in the IEEE 30 system obtained by ABC with the same population size of 100, but only after 600 iterations.

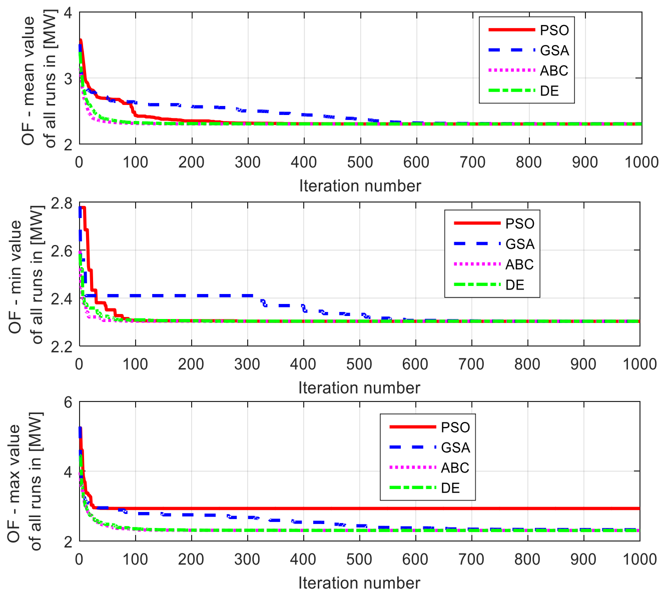

Figure 4. OF convergence—Max, Min, and Mean of all runs for the IEEE 9 test system.

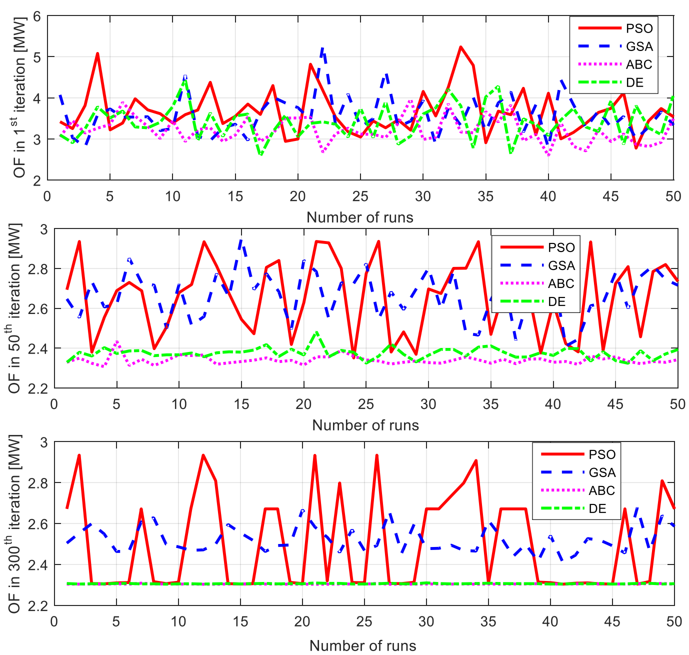

(**a**)

Figure 5. *Cont.*

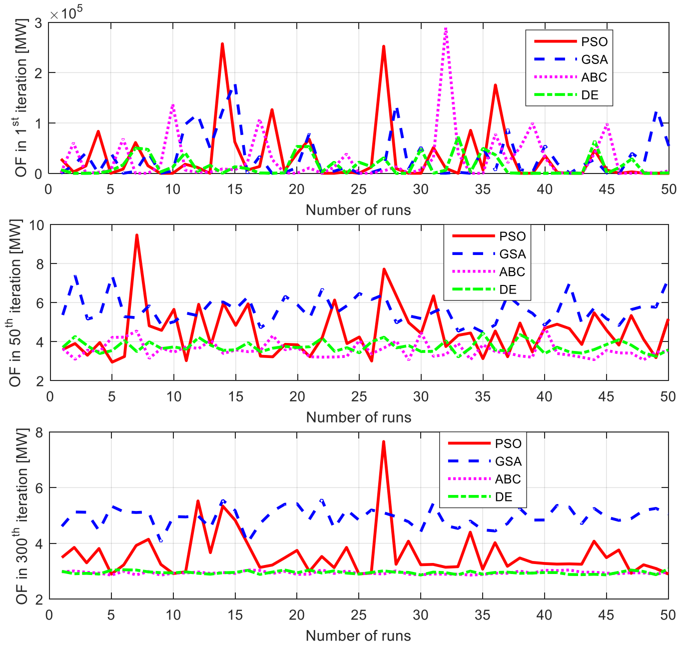

(**b**)

Figure 5. OF in 1st, 50th, and 300th iteration at PSO, GSA, ABC, and DE algorithms' multiple runs, (**a**) IEEE 9 test bus system, (**b**) IEEE 30 test bus system.

Table 1. Comparison of the algorithms regarding the best solution, the number of iterations needed to achieve the best solution, and computation time.

	Best Solution—P_{loss} [MW]		**Iterations**		**Computation Time [s]**	
	IEEE 9	**IEEE 30**	**IEEE 9**	**IEEE 30**	**IEEE 9**	**IEEE 30**
PSO	2.317	**3.39**	440	810	10.56	317.5
GSA	2.317	3.220	650	700	16.89	195.5
ABC	2.317	2.995	**240**	**600**	12.24	420
DE	**2.316**	**2.994**	320	750	**8.32**	**247.5**
CONOPT	2.3157972	2.9937435	-	-	0.073	0.092

Considering all the comparisons of the different metaheuristics shown above, the CONOPT solver embedded in GAMS gave 2.9937435 MW in total power losses, which is a slightly better result for a single objective OPF. Therefore, a CONOPT solver embedded in GAMS can be a usable, reliable, and efficient tool for solving optimal power flow problems.

5. Impact of SVC Location—Simulation Results

The impact of SVC location on power system losses has been analyzed through the following case scenarios:

- CASE 1—system supply constant load;
- CASE 2—system supply variable load;
- CASE 3—system supply variable load in the presence of a fixed wind generator location; and
- CASE 4—system supply variable load for different wind generator locations.

All results are presented for both IEEE 9 and IEEE 30 test bus systems. A variable load data profile is taken from [45] and wind profile data are taken from [65]. In each analyzed case, the OPF is first handled to obtain the minimal value of power losses when there are no SVC devices in the system.

5.1. CASE 1

The results of OPF for the minimization of power system losses when there are no SVC devices in the system are presented in Tables 2 and 3 for the IEEE 9 and IEEE 30 test bus systems, respectively. After that, the optimal value of the SVC's reactive power that minimizes power system losses were tested in all non-generator nodes of this network. All obtained results are presented in the mentioned Tables 2 and 3 as well.

Table 2. Power losses (MW) without and with SVC in the IEEE 9 test bus system—CASE 1.

		Losses [MW]
Without SVC-a		**2.3157972**
SVC in Node:	**Losses [MW]**	**Optimal Value of SVC Devices—Q_{SVC} in [MVAr]**
4	2.3029	31.962
5	2.3082	7.811
6	2.3157	28.347
7	2.3033	16.992
8	2.3157	48.066
9	**2.2429**	**28.504**

Table 3. Power losses (MW) without and with SVC in the IEEE 30 test bus system—CASE 1.

Without SVC	**3.1361950 [MW]**							
SVC in Node:	**Losses [MW]**	**Q_{SVC} [MVAr]**	**SVC in Node:**	**Losses [MW]**	**Q_{SVC} [MVAr]**	**SVC in Node:**	**Losses [MW]**	**Q_{SVC} [MVAr]**
3	3.1283570	7.88470	15	3.0790903	12.11422	23	3.0615291	9.28462
4	3.1102065	20.22564	16	3.1164431	6.32258	**24**	**2.9937435**	**13.83753**
6	3.0935250	30.53385	17	3.0808191	12.75020	25	3.0782495	7.47845
7	3.1051779	13.46546	18	3.0849214	7.83266	26	3.0832614	3.83518
9	3.0595039	35.83722	19	3.0753885	8.64813	27	3.1104100	7.02192
10	3.0663123	23.01893	20	3.0824500	8.70667	28	3.1103671	13.42805
12	3.1361950	9.94304	21	3.0117611	19.28986	29	3.1100272	3.54662
14	3.1270511	3.33737	22	3.0215217	18.06944	30	3.1036651	3.66248

In this case, for the IEEE 9 test bus system, the SVC device was found to be optimally located in node 9, and for IEEE 30 test bus system, in node 24. The minimal value of the power system losses is 2.2429 MW for the IEEE 9 test bus system and 2.9937 MW for the IEEE 30 test bus system, which is a lower value than that of the power system losses for a power system without an SVC device. Therefore, with SVC devices, the power system's efficiency can be improved. For the IEEE 9 test bus system the reduction of power system losses is about 3%, while for IEEE 30 test bus system it is about 4%. In this case, during an optimization process the value of the reactive power of SVC devices was not limited. Hence, the optimized value of the SVC reactive power for some nodes is very high in comparison with others.

The calculation of the SVC reactive power for the minimization of power system losses when the maximal available SVC reactive power is limited is presented in Tables 4 and 5 for both IEEE 9 and IEEE 30 test bus systems, respectively. Evidently, the limitation of the upper limit of the SVC reactive power do not have a high impact on the power system losses. If the SVC reactive power is limited to 10 MVAr in the case of a IEEE 9 test system, the minimal power system losses are 2.2699 MW, which is very close to the optimal value of an SVC reactive power for minimal power system losses (2.2429 MW). For a higher value of the SVC limited reactive power, the power system losses are closer to optimal solution (see the results for node 9 presented in bold). A similar conclusion can be derived for the IEEE 30 test bus system. If the SVC reactive power is limited to 10 MVAr, the minimal power losses are 3.004 MW, while the power losses are 2.9937453 MW when there is no limitation set on the SVC reactive power.

Table 4. Power losses (MW) with SVC in the IEEE 9 test bus system with a limited value of Q_{SVC}—CASE 1.

	Q_{SVCmax} = 10 [MVAr]		Q_{SVCmax} = 15 [MVAr]		Q_{SVCmax} = 20 [MVAr]	
SVC in Node:	**Losses [MW]**	**Optimal Value of Q_{SVC} in [MVAr]**	**Losses [MW]**	**Optimal Value of Q_{SVC} in [MVAr]**	**Losses [MW]**	**Optimal Value of Q_{SVC} in [MVAr]**
4	2.3029	8.6	2.3029	8.6	2.3029	20.0
5	2.3082	7.8	2.3082	7.8	2.3082	7.8
6	2.3157	−4.1	2.3157	−5.5	2.3157	−6.9
7	2.3054	10.0	2.3035	15.0	2.3033	17.0
8	2.3157	10.0	2.3157	15.0	2.3157	20.0
9	**2.2699**	10.0	**2.2562**	15.0	**2.2482**	20.0
	Q_{SVCmax} = 25 [MVAr]		Q_{SVCmax} = 30 [MVAr]		Q_{SVCmax} = 35 [MVAr]	
SVC in Node:	**Losses [MW]**	**Optimal Value of Q_{SVC} in [MVAr]**	**Losses [MW]**	**Optimal Value of Q_{SVC} in [MVAr]**	**Losses [MW]**	**Optimal Value of Q_{SVC} in [MVAr]**
4	2.3029	25.0	2.3029	30.0	2.3029	11.2
5	2.3082	7.8	2.3082	7.8	2.3082	7.8
6	2.3157	−8.3	2.3157	−9.7	2.3157	−23.3
7	2.3033	17.0	2.3033	17.0	2.3033	17.0
8	2.3157	25.0	2.3157	30.0	2.3157	−4.4
9	**2.2438**	25.0	**2.2429**	28.5	**2.2429**	28.5

The impact of SVC reactive power, when located in the optimal node, on the power system losses is presented in Figure 6 for the IEEE 9 test bus system and in Figure 7 for the IEEE 30 test bus system. In these Figures 6 and 7, the results obtained in [22] are also presented. As can be seen, the CONOPT solver embedded in GAMS gave different power system losses in comparison with the results presented in [22]. The results obtained by using the CONOPT solver in systems without SVC devices, for both observed power systems, correspond to the results of OPF presented in [27]. Hence, the optimal placement of SVC devices obtained by using the CONOPT solver are achieved with a higher accuracy compared to the Newton–Raphson method [22]. Note that the results presented in [22] are obtained by using the classic Newton–Raphson method, which has several drawbacks (e.g., it requires accurate initial value, the function and its derivatives must be continuous on the range you search, etc.), unlike the usage of a CONOPT solver [26].

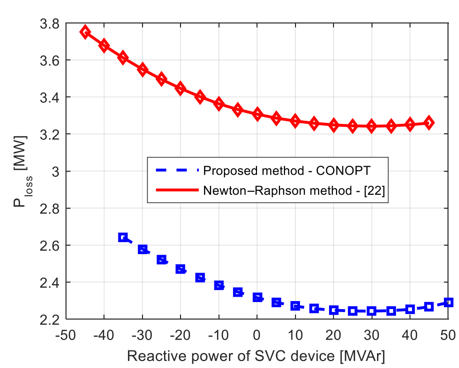

Figure 6. The impact of the reactive power of SVC devices located in node 9 on power system losses in the IEEE 9 test bus system.

Table 5. Power losses (MW) with SVC in the IEEE 30 test bus system with a limited value of Q_{SVC}—CASE 1.

	Q_{SVCmax} = 10 [MVAr]		Q_{SVCmax} = 20 [MVAr]		Q_{SVCmax} = 30 [MVAr]	
SVC in Node:	**Losses [MW]**	**Q_{SVC} [MVAr]**	**SVC in Node:**	**Losses [MW]**	**Q_{SVC} [MVAr]**	**SVC in Node:**
3	3.128	7.9	3.128	7.9	3.128	7.9
4	3.116	10.0	3.110	20.0	3.110	20.2
6	3.112	10.0	3.098	20.0	3.093	30.0
7	3.107	10.0	1.105	13.5	3.105	13.5
9	3.103	10.0	3.080	20.0	3.064	30.0
10	3.088	10.0	3.067	20.0	3.066	23.0
12	3.136	10.0	3.136	14.2	3.136	30.0
14	3.127	3.33	3.127	3.33	3.127	3.33
15	3.080	10.0	3.079	12.1	3.079	12.1
16	3.116	6.32	3.116	6.32	3.116	6.32
17	3.083	10.0	3.080	12.8	3.080	12.8
18	3.084	7.83	3.084	7.83	3.084	7.83
19	3.075	8.64	3.075	8.64	3.075	8.64
20	3.082	8.7	3.082	8.7	3.082	8.7
21	3.039	10.0	3.011	19.3	3.011	19.3
22	3.043	10.0	3.021	18.1	3.021	18.1
23	3.061	9.28	3.061	9.28	3.061	9.28
24	**3.004**	**10.0**	**2.994**	**13.8**	**2.994**	**13.8**
25	3.078	7.47	3.078	7.47	3.078	7.47
26	3.083	3.83	3.083	3.83	3.083	3.83
27	3.110	7.02	3.110	7.02	3.110	7.02
28	3.112	10.0	3.110	13.4	3.110	13.4
29	3.110	3.54	3.110	3.54	3.110	3.54
30	3.103	3.66	3.103	3.66	3.103	3.66

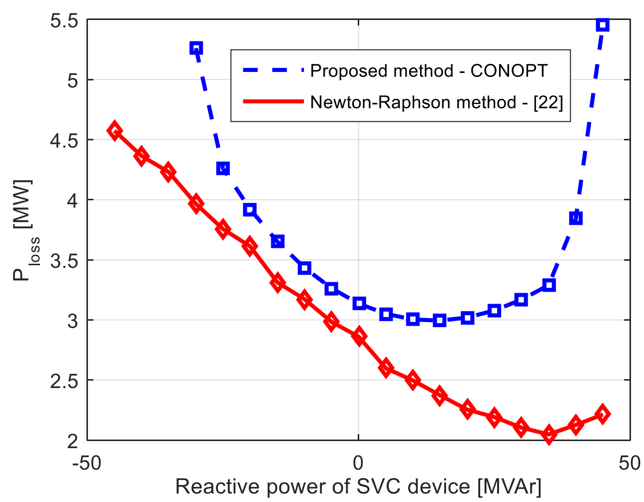

Figure 7. The impact of the reactive power of SVC devices located in node 24 on power system losses in the IEEE 30 test bus system.

5.2. CASE 2

In this case, the optimal location and optimal reactive power of SVC devices to minimize the power system losses when the system supplies a variable load was determined. The load variation is given in Figure 8 [45]. Firstly, the results of OPF for power system minimization of power system losses, in the case when there are no SVC devices in the system, are presented in Tables 6 and 7 for both analyzed networks, respectively. All non-generator nodes of these networks were tested to find the optimal value of SVC's reactive power that minimizes power system losses. The summarized obtained results are also presented in Tables 6 and 7 for both networks.

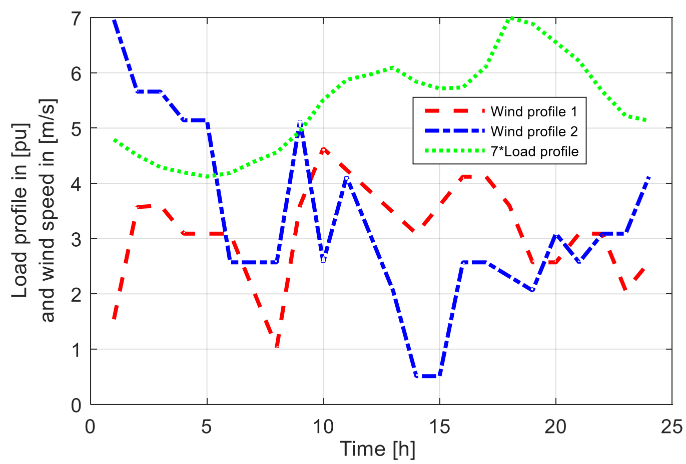

Figure 8. Load and wind speed profiles.

Table 6. Power losses (MW) without and with SVC in the IEEE 9 test bus system—CASE 2.

	Power Losses [MW]
Without SVC	**33.203**
SVC in Node:	**Power Losses [MW]**
4	33.175
5	33.065
6	33.203
7	33.120
8	33.203
9	**32.726**

Table 7. Power losses (MW) without and with SVC in the IEEE 30 test bus system—CASE 2.

Without SVC			**39.048 [MW]**		
SVC in Node:	**Power Losses [MW]**	**SVC in Node:**	**Power Losses [MW]**	**SVC in Node:**	**Power Losses [MW]**
3	38.986	14	38.926	22	37.647
4	38.783	15	38.324	23	38.097
5	39.048	16	38.815	24	37.246
6	38.627	17	38.409	25	38.388
7	38.703	18	38.405	26	38.393
9	38.238	19	38.292	27	38.831
10	38.285	20	38.397	28	38.805
12	39.048	21	37.516	29	38.774
				30	38.693

The optimal location of an SVC is node 9 in the IEEE 9 test bus system (minimal power losses are 32.726 MW) and node 24 in the IEEE 30 test bus system (minimal power losses are 37.246 MW). If there is an SVC device in the system, power losses are lower than if there is no SVC device. Power losses are about 0.5 MW lower in the IEEE 9 test bus system and about 1.8 MW lower in the IEEE 30 test bus system. Therefore, for the IEEE 9 test bus system, reduction in power system losses is very small (about 1.5%), while for the IEEE 30 test bus system, it is about 4.1%. Figure 9 presents the power losses versus time (without SVC in the network and with SVC in the optimal node), the reactive power of an SVC device connected in the optimal node versus time, and 3D graphs (node number-time-reactive power) for the IEEE 9 and IEEE 30 test bus systems.

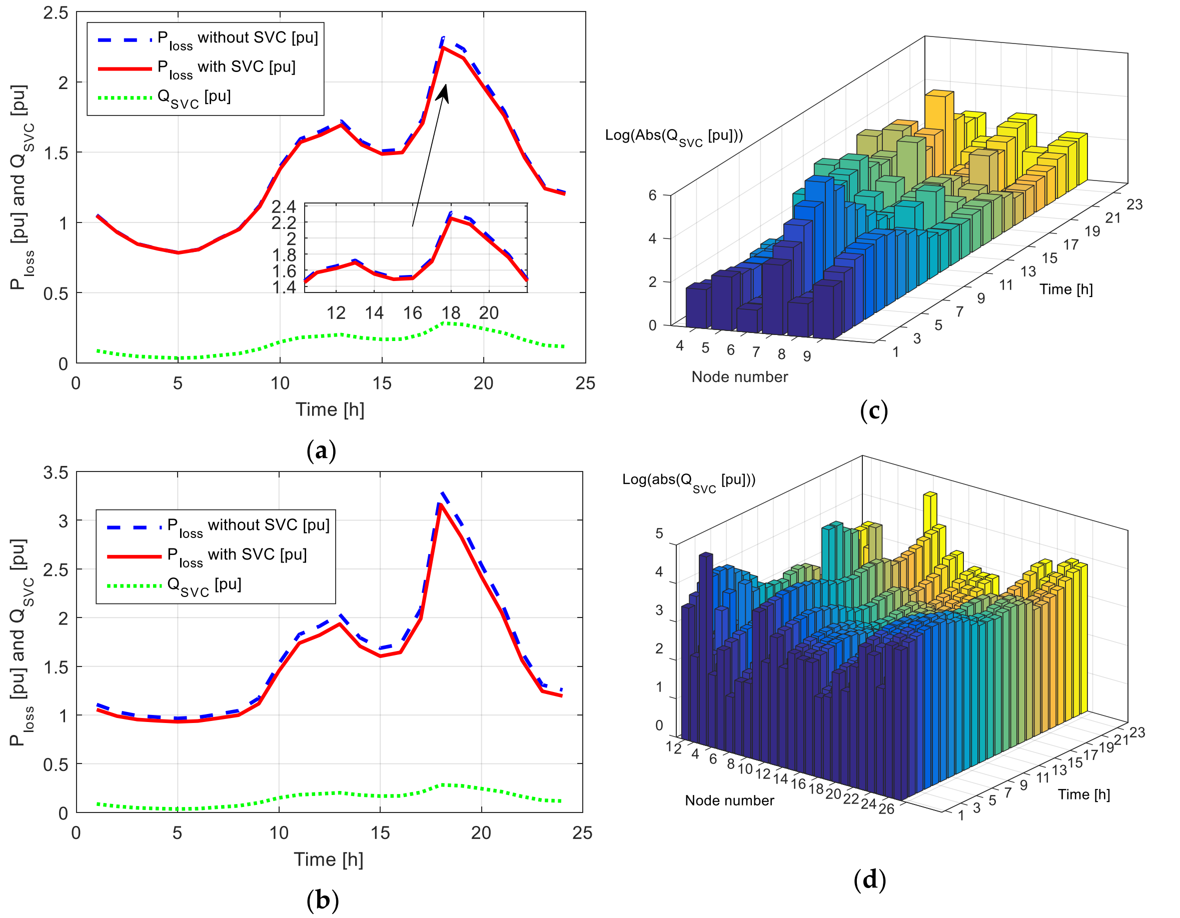

Figure 9. Power losses and reactive power of an SVC device connected in the optimal node for (**a**) IEEE 9 and (**b**) IEEE 30 test bus system, as well as 3D graphs (node number-time-reactive power) for (**c**) IEEE 9 and (**d**) IEEE 30 test bus systems.

As can be seen, SVC has the highest impact in time step around maximal power load (Figure 9a,b. The reactive power of an SVC device changes during a day (for optimal node its maximal value is at maximal value of load), as well as for different nodes. During the previously mentioned optimization, the value of Q_{svc} was not limited, and therefore it is evident that in some period of the observed interval, a very high value of Q_{svc} is required.

5.3. CASE 3

This case deals with the optimal location of SVC devices in power networks that contain one wind generator. For both test systems, a 15 MW wind generator was connected in node 5. The wind speed profile and load profile are given in Figure 8 (wind profile 1). The wind power P_{w} was calculated according to the following expression:

$$P_w = \begin{cases} 0 & w_t < w_{CI} \quad \text{or} \quad w_t \geq w_{CO} \\ P_w^{\max} \frac{w_t - w_{CI}}{w_R - w_{CI}} & w_{CI} \leq w_t < w_R \\ P_w^{\max} & w_R \leq w_t < w_{CO} \end{cases} \tag{12}$$

where $P_w^{\max}$ represents the rated wind power, while w_t, w_{CI}, w_{CO}, and w_R are the wind speed at hour t, cut-in wind speed, cut-out wind speed, and rated wind speed, respectively. Figure 10 shows wind power versus wind speed characteristics. In this paper $w_{CI} = 1$ m/s , $w_{CO} = 11$ m/s and $w_R = 4$ m/s.

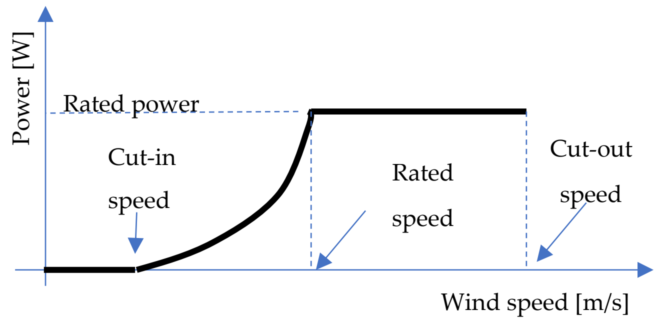

Figure 10. Typical wind power versus wind speed curve.

The procedure to determine the optimal node for SVC is the same as in CASE 2. The obtained results of OPF for the minimization of power losses in systems where SVC devices are not included are presented in Table 8, and Table 9, for the IEEE 9 and IEEE 30 test bus systems, respectively.

Table 8. Power losses (MW) without and with SVC in the IEEE 9 test bus system—CASE 3.

	Power Losses [MW]
Without SVC	**31.102**
SVC in Node:	**Power Losses [MW]**
4	31.081
6	31.102
7	31.020
8	31.102
9	**30.630**

Table 9. Power losses (MW) without and with SVC in the IEEE 30 test bus system—CASE 3.

Without SVC			**36.972 [MW]**		
SVC in Node:	**Power Losses [MW]**	**SVC in Node:**	**Power Losses [MW]**	**SVC in Node:**	**Power Losses [MW]**
3	36.911	15	36.252	23	36.025
4	36.709	16	36.741	**24**	**35.176**
6	36.558	17	36.338	25	36.315
7	36.634	18	36.332	26	36.319
9	36.170	19	36.219	27	36.757
10	36.213	20	36.324	28	36.732
12	36.972	21	35.445	29	36.699
14	36.851	22	35.576	30	36.619

After that, all non-generator nodes of these networks were tested to find the optimal value of SVC's reactive power that minimizes power system losses. The obtained results are also summarized in Tables 8 and 9 for both networks. In the IEEE 9 test bus system with a wind generator, the optimal SVC location is in node 9. In this case, the minimal power system losses are 30.63 MW, which is about 0.5 MW lower than in the case that there is no SVC device. It can be concluded that for the IEEE 9 test bus system, the increase in the power system efficiency is very small.

In the IEEE 30 test bus system, the optimal SVC location is in node 24, and the minimal value of losses is 35.176 MW, which is about 1.7 MW lower than in the case that there is no SVC device. Thus, the reduction of power system losses is about 4.5%. In this case, the optimal SVC location is the same as that presented in CASE 2 (variable load without renewables). The power losses versus time (without SVC in the network and with SVC in optimal node), reactive power of SVC device connected in the optimal node versus time, and 3D graph (node number-time-reactive power) for IEEE 9 and IEEE 30 test bus systems, when they contain a 15 MW generator, are presented in Figure 11. Observing the 3D graphs presented in Figure 11, it is evident that the wind generator has a significant impact on the SVC reactive power profile during the day, for any observed node. Note that, as in CASE 2, during the optimization the value of Q_{SVC} was not limited.

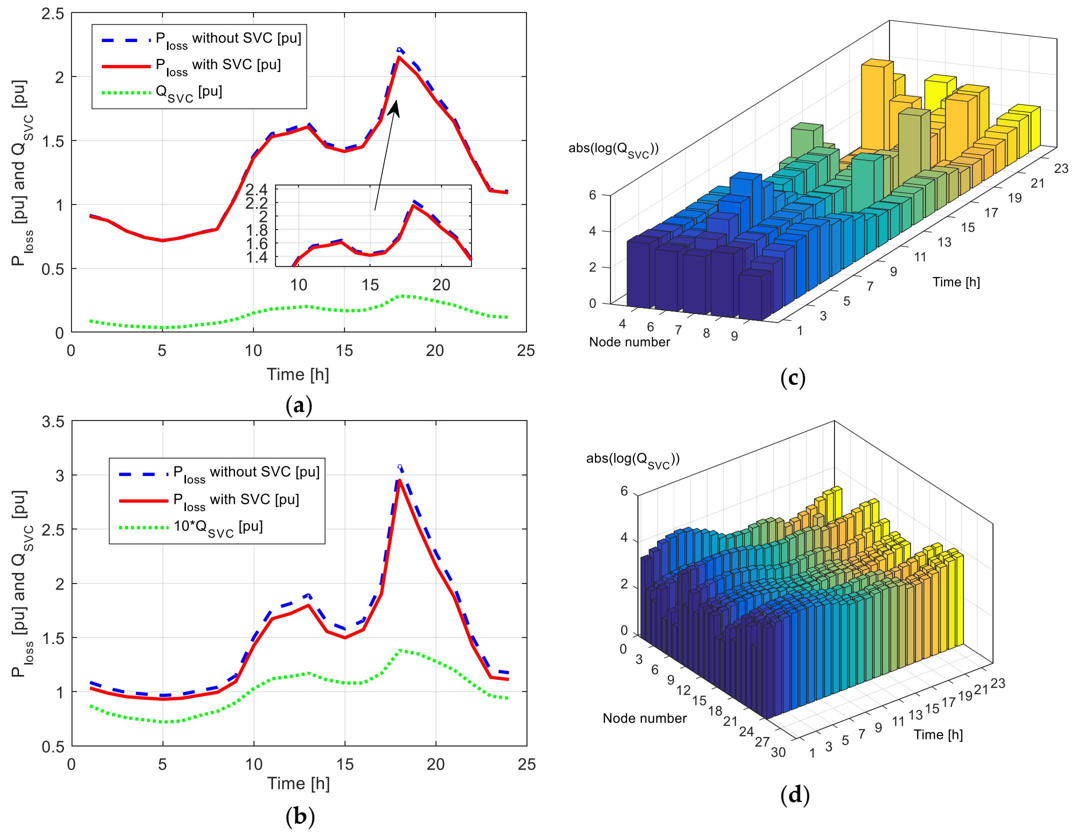

Figure 11. Power losses and reactive power of SVC device connected in the optimal node for (**a**) IEEE 9 and (**b**) IEEE 30 test bus system, as well as 3D graphs (node number-time-reactive power) for (**c**) IEEE 9 and (**d**) IEEE 30 test bus systems with a wind generator.

5.4. CASE 4

In this section, the impact of the locations of the wind power generator and SVC device on the power system losses are tested. Namely, the optimal location of SVC devices is observed for all possible wind generator positions. For this goal, the modified IEEE 9 test bus system is observed. Also, two different wind profiles are analyzed. The wind data are taken for the city of Dharan, Nepal [65], for data 01.12.2019 and 05.01.2020. Unlike the analysis in Case 3, the rated power of the wind generator is 70 MW. During the optimization process, the maximum value of the SVC reactive power was limited to 20 MVAr. The obtained results are presented in Table 10.

Table 10. Power system losses in the case of a wind generator and different SVC connections.

Wind Generator in Node 4			Wind Generator in nOde 5			Wind Generator in Node 6		
	Wind Profile 1	**Wind Profile 2**		**Wind Profile 1**	**Wind Profile 2**		**Wind Profile 1**	**Wind Profile 2**
Without SVC	**33.573**	**33.600**	**Without SVC**	**25.993**	**25.178**	**Without SVC**	**33.466**	**34.228**
SVC in Node:	**Power Losses [MW]**	**Power Losses [MW]**	**SVC in Node:**	**Power Losses [MW]**	**Power Losses [MW]**	**SVC in Node:**	**Power Losses [MW]**	**Power Losses [MW]**
4	33.438	33.465	5	25.983	25.172	4	33.440	34.202
6	33.573	33.600	6	25.993	25.178	5	33.325	34.091
7	33.488	33.515	7	25.908	25.093	7	33.381	34.142
8	33.573	33.600	8	25.993	25.178	8	33.466	34.228
9	**33.107**	**33.133**	**9**	**25.528**	**24.715**	**9**	**32.989**	**33.752**
Wind Generator in Node 7			**Wind Generator in Node 8**			**Wind Generator in Node 9**		
	Wind Profile 1	**Wind Profile 2**		**Wind Profile 1**	**Wind Profile 2**		**Wind Profile 1**	**Wind Profile 2**
Without SVC	**29.581**	**29.072**	**Without SVC**	**33.285**	**33.683**	**Without SVC**	**25.688**	**24.300**
SVC in Node:	**Power Losses [MW]**	**Power Losses [MW]**	**SVC in Node:**	**Power Losses [MW]**	**Power Losses [MW]**	**SVC in Node:**	**Power Losses [MW]**	**Power Losses [MW]**
4	29.555	29.046	4	33.259	33.656	4	25.680	24.297
5	29.443	28.934	5	33.146	33.546	**5**	**25.559**	**24.174**
6	29.581	29.072	6	33.285	33.683	6	25.688	24.300
8	29.581	29.072	7	33.200	33.597	7	25.603	24.215
9	**29.104**	**28.595**	**9**	**32.809**	**33.208**	8	25.688	24.300

These results can be summarized as follows:

- For both wind profiles, when there are no SVC devices, the optimal location of the wind generator is node 9.
- When the wind generator is connected in nodes 4, 5, 6, 7, or 8 for both wind profiles, the optimal location of SVC device is node 9. When the wind generator is connected in node 9 for both wind profiles, the optimal location of the SVC device is node 5.
- Finally, for wind profile 1, the minimal losses can be obtained if the wind generator is connected in node 5, and SVC in node 9 (25.528 MW). For wind profile 2, the minimal losses can be obtained if the wind generator is connected in node 9, and SVC in node 5 (24.174 MW).

Based on the presented results, as well as the literature review, a comparison of the different approaches is presented in Table 11. It can be concluded that the problem of optimal SVC allocation in power systems has been considered taking into account different test systems with and without renewable power sources, optimization methods, and other criteria.

Table 11. Comparison of different approaches for optimal SVC allocation.

	IEEE Test Bus System	Power System with Renewables	Optimization Method	Criteria
Proposed method	9, 30	Yes	CONOPT solver	power loss minimization
Mondal, 2012 [4]	14	Yes	PSO	signal stability problem
Huang, 2013 [8]	30	No	GA	loadability
Basiri-Kejani, 2016 [11]	Isfahan–Khuzestan power system	No	HICAGA	loadability, power system losses, total voltage deviations SVC installation cost
Ray, 2018, [12]	30, 57	No	WOA, DE, GWO, QODE, QOGWO	voltage collapse proximity indication
Mahdad, 2016 [13]	33, 69	Yes	DS	power loss minimization
Belati, 2019 [14]	118		branch and bound algorithm	voltage profile Power loss minimization
Savić, 2014 [15]	distribution network	Yes	GA	Voltage deviations
Xu, 2018, [16]	distribution network	Yes	-	Investment cost
Benabid, 2009, [19]	30-bus Algerian 114-bus power system	No	PSO	Voltage stability
Singh, 2018 [22]	9, 30	No	Newton–Raphson method	Voltage profile Power loss minimization

6. Conclusions

This paper deals with the improvement of power system efficiency using SVC devices. Although this solution is known in the literature, in this paper the optimal SVC location was optimized using a CONOPT solver embedded in GAMS, which was not seen in the literature before. Two test systems (IEEE 9 and IEEE 30), with and without wind generators were observed and analyzed through 4 different cases: system supply constant load, variable load, variable load in the presence of a fixed wind generator location, and variable load for different wind generator locations. It was shown that the wind profile, power of wind generator, and location of the wind generator (connection to networks) all have a significant impact on power system losses regarding the usage of SVC devices. Based on our knowledge and our review of the literature, a CONOPT solver embedded in GAMS was used for the first time for optimal SVC allocation in the abovementioned cases.

Furthermore, based on obtained results that were compared with known solutions from the literature, it can be concluded that the CONOPT solver is suitable and effective for finding the optimal SVC location. Also, the use of the CONOPT solver for optimal power flow problem solving over metaheuristic methods was investigated. It was shown that the CONOPT solver is more accurate than classical methods, and more efficient and reliable in comparison with metaheuristics methods.

In our future work, attention will be paid to the both economic and technical aspects of installing SVC devices in grids. Also, attention will be paid to the mutual impact of the device for reactive power compensation and devices for power energy storage to minimize power system losses and power production costs.

Author Contributions: Conceptualization, M.Ć. and T.K.; Methodology, M.Ć.; software, K.K. and L.N.; validation, T.K and M.Ć., formal analysis, M.Ć.; investigation, M.Ć. and T.K.; resources, M.Ć.; writing—original draft preparation, M.Ć. and T.K.; writing—review and editing, T.K.; visualization, M.Ć.; supervision, M.Ć. All authors have read and agreed to the published version of the manuscript.

Funding: This research received no external funding.

Conflicts of Interest: The authors declare no conflict of interest.

References

1. Ismael, S.M.; Aleem, S.H.A.; Abdelaziz, A.Y.; Zobaa, A.F. State-of-the-art of hosting capacity in modern power systems with distributed generation. *Renew. Energy* **2019**, *130*, 1002–1020. [CrossRef]
2. Dixon, J.; Moran, L.; Rodriguez, J.; Domke, R. Reactive Power Compensation Technologies: State-of-the-Art Review. *Proc. IEEE* **2005**, *93*, 2144–2164. [CrossRef]
3. Nadeem, M.; Imran, K.; Khattak, A.; Ulasyar, A.; Pal, A.; Zeb, M.Z.; Khan, A.N.; Padhee, M. Optimal Placement, Sizing and Coordination of FACTS Devices in Transmission Network Using Whale Optimization Algorithm. *Energies* **2020**, *13*, 753. [CrossRef]
4. Mondal, D.; Chakrabarti, A.; Sengupta, A. Optimal placement and parameter setting of SVC and TCSC using PSO to mitigate small signal stability problem. *Int. J. Electr. Power Energy Syst.* **2012**, *42*, 334–340. [CrossRef]
5. Chang, C.S.; Qizhi, Y. Fuzzy bang–bang control of static VAR compensators for damping system-wide low-frequency oscillations. *Electr. Power Syst. Res.* **1999**, *49*, 45–54. [CrossRef]
6. Hemeida, M.G.; Hegazy, R.; Mohamed, M.H. A comprehensive comparison of STATCOM versus SVC-based fuzzy controller for stability improvement of wind farm connected to multi-machine power system. *Electr. Eng.* **2017**, *99*, 1–17. [CrossRef]
7. Darabian, M.; Jalilvand, A. A power control strategy to improve power system stability in the presence of wind farms using FACTS devices and predictive control. *Int. J. Electr. Power Energy Syst.* **2017**, *85*, 50–66. [CrossRef]
8. Huang, J.S.; Jiang, Z.H.; Negnevitsky, M. Loadability of power systems and optimal SVC placement. *Int. J. Electr. Power Energy Syst.* **2013**, *45*, 167–174. [CrossRef]
9. Ghahremani, E.; Kamwa, I. Optimal placement of multiple-type FACTS devices to maximize power system loadability using a generic graphical user interface. *IEEE Trans. Power Syst.* **2013**, *28*, 764–778. [CrossRef]
10. Gerbex, S.; Cherkaoui, R.; Germond, A.J. Optimal location of multi-type FACTS devices in a power system by means of genetic algorithms. *IEEE Trans. Power Syst.* **2001**, *16*, 537–544. [CrossRef]
11. Basiri-Kejani, M.; Gholipour, E. Two-level procedure based on HICAGA to determine optimal number, locations and operating points of SVCs in Isfahan–Khuzestan power system to maximise loadability and minimise losses, TVD and SVC installation cost. *IET Gener. Transm. Distrib.* **2016**, *10*, 4158–4168. [CrossRef]
12. Raj, S.; Bhattacharyya, B. Optimal placement of TCSC and SVC for reactive power planning using Whale optimization algorithm. *Swarm Evol. Comput.* **2018**, *40*, 131–143. [CrossRef]
13. Mahdad, B.; Srairi, K. Adaptive differential search algorithm for optimal location of distributed generation in the presence of SVC for power loss reduction in distribution system. *Int. J. Eng. Sci. Technol.* **2016**, *19*, 1266–1282. [CrossRef]

14. Belati, E.A.; Nascimento, C.F.; de Faria, H.; Watanabe, E.H.; Padilha-Feltrin, A. Allocation of Static Var Compensator in Electric Power Systems Considering Different Load Levels. *J. Control Autom Electr. Syst.* **2019**, *30*, 1–8. [CrossRef]
15. Savić, A.; Djurišić, Ž. Optimal sizing and location of SVC devices for improvement of voltage profile in distribution network with dispersed photovoltaic and wind power plants. *Appl. Energy* **2014**, *134*, 114–124. [CrossRef]
16. Xu, X.; Xu, Z.; Lyu, X.; Li, J. Optimal SVC placement for Maximizing Photovoltaic Hosting Capacity in Distribution Network. *IFAC-Pap. Online* **2018**, *51*, 356–361. [CrossRef]
17. Elmitwally, A.; Eladl, A. Planning of multi-type FACTS devices in restructured power systems with wind generation. *Int. J. Electr. Power Energy Syst.* **2016**, *77*, 33–42. [CrossRef]
18. Duan, C.; Fang, W.; Jiang, L.; Niu, S. FACTS Devices Allocation via Sparse Optimization. *IEEE Trans. Power Syst.* **2016**, *31*, 1308–1319. [CrossRef]
19. Benabid, R.; Boudour, M.; Abido, M.A. Optimal location and setting of SVC and TCSC devices using non-dominated sorting particle swarm optimization. *Electr. Power Syst. Res.* **2009**, *79*, 1668–1677. [CrossRef]
20. Jordehi, A.R. Brainstorm optimisation algorithm (BSOA): An efficient algorithm for finding optimal location and setting of FACTS devices in electric power systems. *Int. J. Electr. Power Energy Syst.* **2015**, *69*, 48–57. [CrossRef]
21. Ahmad, A.A.; Sirjani, R. Optimal placement and sizing of multi-type FACTS devices in power systems using metaheuristic optimisation techniques: An updated review. *Ain Shams Eng. J.* **2019**, in press. [CrossRef]
22. Singh, B.; Agrawal, G. Enhancement of voltage profile by incorporation of SVC in power system networks by using optimal load flow method in MATLAB/Simulink environments. *Energy Rep.* **2018**, *4*, 418–434. [CrossRef]
23. Sebaa, K.; Bouhedda, M.; Tlemcani, A.; Henini, N. Location and tuning of TCPSTs and SVCs based on optimal power flow and an improved cross-entropy approach. *Int. J. Electr. Power Energy Syst.* **2014**, *54*, 536–545. [CrossRef]
24. Subasri, C.K.; Charles Raja, S.; Venkatesh, P. Power quality improvement in a wind farm connected to grid using FACTS device. *Power Electron Renew Energy Syst.* **2015**, *326*, 1203–1212.
25. Liao, H.; Milanović, J. On capability of different FACTS devices to mitigate a range of power quality phenomena. *IET Gener. Transm. Distrib.* **2017**, *11*, 2002–2012. [CrossRef]
26. Ćalasan, M.P.; Nikitović, L.; Mujović, S. CONOPT solver embedded in GAMS for optimal power flow. *J. Renew. Sustain. Energy* **2019**, *11*, 046301. [CrossRef]
27. Warid, W.; Hizam, H.; Mariun, N.; Abdul-Wahab, N.I. Optimal Power Flow Using the Jaya Algorithm. *Energies* **2016**, *9*, 678. [CrossRef]
28. Reddy, S.S.; Panigrahi, B.K. Optimal power flow using clustered adaptive teaching learning-based optimization. *Int. J. Bio-Inspired Comput.* **2017**, *9*, 226–234. [CrossRef]
29. Adaryani, R.; Karami, M.A. Artificial bee colony algorithm for solving multiobjective optimal power flow problem. *Int. J. Electr. Power Energy Syst.* **2013**, *53*, 219–230. [CrossRef]
30. Liang, R.H.; Tsai, S.R.; Chen, Y.T.; Tseng, W.T. Optimal power flow by a fuzzy based hybrid particle swarm optimization approach. *Electr Power Syst. Res.* **2011**, *81*, 1466–1474. [CrossRef]
31. Kecojević, K.; Lukačević, O.; Ćalasan, M. Impact of static var compensator (SVC) devices on power system losses. *BH Electr. Eng.* **2019**, *13*, 50–55.
32. He, L.; Wei, Z.; Yan, H.; Xv, K.Y.; Zhao, M.Y.; Cheng, S. A Day-ahead Scheduling Optimization Model of Multi-Microgrid Considering Interactive Power Control. In Proceedings of the 4th International Conference on Intelligent Green Building and Smart Grid (IGBSG), Yi-chang, China, 6–9 September 2019; pp. 666–669.
33. Chiu, W.Y.; Sun, H.; Poor, H.V. A Multiobjective Approach to Multimicrogrid System Design. *IEEE Trans. Smart Grid* **2015**, *6*, 2263–2272. [CrossRef]
34. Zheng, X.; Cao, H.; Li, H.; Cui, T.; Jiang, Y.; Zhang, M. Multi-inverters Pre-synchronization VSG Control Strategy for the Microgrid System. In Proceedings of the IEEE 4th International Future Energy Electronics Conference (IFEEC), Singapore, 25–28 November 2019; pp. 1–5.
35. Mohanty, A.; Viswavandya, M.; Ray, P.K.; Patra, S. Stability analysis and reactive power compensation issue in a microgrid with a DFIG based WECS. *Electr. Power Energy Syst.* **2014**, *62*, 753–762. [CrossRef]

36. Gabbar, H.A.; Abdelsalam, A.A. Microgrid energy management in grid-connected and islanding modes based on SVC. *Energy Convers. Manag.* **2014**, *86*, 964–972. [CrossRef]
37. Abdelsalam, A.A.; Gabbar, H.A.; Sharaf, A.M. Performance enhancement of hybrid AC/DC microgrid based D-FACTS. *Int. J. Electr. Power Energy Syst.* **2015**, *67*, 298–323. [CrossRef]
38. Mithulananthan, N.; Canizares, C.A.; Reeve, J.; Rogers, G.J. Comparison of PSS, SVC, and STATCOM Controllers for Damping Power System Oscillations. *IEEE Trans. Power Syst.* **2003**, *18*, 786–792. [CrossRef]
39. Mithulananthan, N.; Canizares, C.A.; Reeve, J.; Rogers, G.J. New Coordinated Design of SVC and PSS for Multi-machine Power System Using BF-PSO Algorithm. *Procedia Technol.* **2013**, *11*, 65–74.
40. Kundur, P. *Power System Stability and Control*; McGraw-Hill: Toronto, ON, Canada, 1994.
41. Benaissa, M.O.; Hadjeri, S.; Zidi, S.A. Impact of PSS and SVC on the Power System Transient Stability. *Adv. Sci. Technol. Eng. Syst.* **2017**, *2*, 562–568. [CrossRef]
42. Yuan, S.Q.; Fang, D.Z. Robust PSS Parameters Design Using a Trajectory Sensitivity Approach. *IEEE Trans. Power Syst.* **2009**, *24*, 1011–1018. [CrossRef]
43. Mutale, J.; Strbac, G. Transmission network reinforcement versus FACTS: An economic assessment. *IEEE Trans. Power Syst.* **2000**, *15*, 961–967. [CrossRef]
44. Lukačević, O.; Ćalasan, M.; Mujović, S. Impact of optimal ESS allocation in IEEE 24-test bus system on total production cost. In Proceedings of the 20th International Symposium POWER ELECTRONICS Ee2019, Novi Sad, Serbia, 23–26 October 2019; pp. 1–5.
45. Soroudi, A. *Power System Optimization Modeling in GAMS*; Springer: Basel, Switzerland, 2017.
46. Duman, S.; Güvenç, U.; Sönmez, Y.; Yörükeren, N. Optimal power flow using gravitational search algorithm. *Energy Convers. Manag.* **2012**, *59*, 86–95. [CrossRef]
47. Bhattacharya, A.; Roy, P.K. Solution of multi-objective optimal power flow using gravitational search algorithm. *IET Gener. Transm. Distrib.* **2012**, *6*, 751–763. [CrossRef]
48. Miranda, V.; Alves, R. Differential Evolutionary Particle Swarm Optimization (DEEPSO): A successful hybrid. In Proceedings of the BRICS Congress on Computational Intelligence & 11th Brazilian Congress on Computational Intelligence, Ipojuca, Brazil, 8–11 September 2019.
49. Chiu, W.Y. Multiobjective controller design by solving a multiobjective matrix inequality problem. *IET Control Theory Appl.* **2014**, *8*, 1656–1665. [CrossRef]
50. Deng, J.; Mao, Y.; Yang, Y. Distribution Power Loss Reduction of Standalone DC Microgrids Using Adaptive Differential Evolution-Based Control for Distributed Battery Systems. *Energies* **2020**, *13*, 2129. [CrossRef]
51. Ebeed, M.; Kamel, S.; Jurado, F. Chapter 7-Optimal Power Flow Using Recent Optimization Techniques. In *Classical and Recent Aspects of Power System Optimization*; Elsevier: Amsterdam, The Netherlands, 2018; ISBN 978-0-12-812441-3.
52. Carpentier, J. Contribution á l'étude du dispatching économique. *Bulletin de la Société Française des Électriciens* **1962**, *8*, 431–447.
53. Frank, S.; Steponavice, I.; Rebennack, S. Optimal power flow: A bibliographic survey I, formulations and deterministic methods. *Energy Syst.* **2012**, *3*, 221–258. [CrossRef]
54. Glover, F. Future paths for integer programming and links to artificial intelligence. *Comput. Oper. Res.* **1986**, *13*, 533–549. [CrossRef]
55. Glover, F.; Kochenberger, G.A. *Handbook of Metaheuristic*; Springer-International Series in Operations Research & Management Science: New York; Kluwer: Philadelphia, PA, USA, 2003.
56. Boussaid, I.; Lepagnot, J.; Siarry, P. A survey on optimization metaheuristic. *Inf. Sci.* **2013**, *237*, 82–117. [CrossRef]
57. Radosavljević, J. *Metaheuristic Optimization in Power Engineering*; IET: London, UK, 2018.
58. Frank, S.; Steponavice, I.; Rebennack, S. Optimal power flow: A bibliographic survey II, Non-deterministic and hybrid methods. *Energy Syst.* **2012**, *3*, 259–289. [CrossRef]
59. Buch, H.; Trivedi, I.N. On the efficiency of the metaheuristics for solving optimal power flow. *Neural Comput. Appl.* **2019**, *31*, 5609–5627. [CrossRef]

60. Narimani, M.R.; Azizipanah-Abarghooee, R.; Zoghdar-Moghadam-Shahrekohne, B.; Gholami, K. A novel approach to multi-objective optimal power flow by a new hybrid optimization algorithm considering generator constraints and multi-fuel type. *Energy* **2013**, *49*, 119–136. [CrossRef]
61. Andrei, N. *Continuous Nonlinear Optimization for Engineering Applications in GAMS Technology*; Springer International Publishing AG: Cham, Switzerland, 2017.
62. Sailaja, M.K.; Maheswarapu, S. Enhanced genetic algorithm based computation technique for multi-objective optimal power flow Solution. *Int. J. Electri. Power* **2010**, *32*, 736–742.
63. Abido, M.A.; Al-Ali, N.A. Multi-objective differential evolution for optimal power flow. In Proceedings of the IEEE International Conference on Power Engineering, Energy and Electrical, Drives, 2009 (POWERENG'09), Lisbon, Portugal, 18–20 March 2009; pp. 101–106.
64. He, X.; Wang, W.; Jiang, J.; Xu, L. An Improved Artificial Bee Colony Algorithm and Its Application to Multi-Objective Optimal Power Flow. *Energies* **2015**, *8*, 2412–2437. [CrossRef]
65. Available online: https://www.windfinder.com/#3/50.2050/18.7646 (accessed on 20 February 2020).